Phase transition of some ferroelectric niobate crystals with tungsten-bronze structure at low temperatures

Yuhuan Xu, Zhongrong Li, Wu Li, and Hong Wang
Department of Physics, Zhongshan University, Guangzhou, China

Huanchu Chen
Institute of Crystal Materials, Shandong University, Jinan, China
(Received 14 December 1988; revised manuscript received 21 June 1989)

From 15 K to room temperature, dielectric and pyroelectric properties have been measured in six ferroelectric niobate single crystals with tungsten-bronze (TB) structure. Dielectric and pyroelectric experiments show that in the three kinds of ferroelectric niobate single crystals $Sr_{1-x}Ba_xNb_2O_6$, $Pb_xBa_{1-x}Nb_2O_6$, and $(K_xNa_{1-x})_{0.4}(Sr_yBa_{1-y})_{0.8}Nb_2O_6$ with tetragonal TB structure, there is a newly identified phase transition between 60 and 80 K which has been supported by x-ray analysis. The crystal's symmetry changes from point group $4mm$ to point group m, and the direction of the ferroelectric polar axis tilts away from the c axis in the tetragonal lattice cell to the a axis in the monoclinic lattice cell as temperature decreases. The difference between the high-frequency dielectric constants and the low-frequency dielectric constants indicates that the phase transition is of a diffuse nature. According to the specific-heat experimental data, it is suggested that this phase transition is not a first-order transition. A model of structural change has been suggested to explain this phase transition.

I. INTRODUCTION

Ferroelectric niobate single crystals with tungsten-bronze (TB) -type structure are a class of important materials for applications in electro-optic, nonlinear optic, and pyroelectric effects. Early studies of the niobate $PbNb_2O_6$ were performed in 1953. Afterwards, it was found that some alkali and alkaline earth metal niobates having TB structure possess fairly good nonlinear optical properties.[1] Among them, $Ba_2NaNb_5O_{15}$ is especially good in the application of frequency multiplication in nonlinear optics, and has no laser damage at room temperature. $Sr_{1-x}Ba_xNb_2O_6$ series of niobate solid solution crystals were found to have excellent electro-optical and pyroelectric properties.[2] Such crystals are used to make modulators, frequency multipliers, and other electro-optical devices. A new, very useful ferroelectric crystal $(K_xNa_{1-x})_{0.4}(Sr_yBa_{1-y})_{0.8}Nb_2O_6$ was developed in 1981,[3-12] and is especially suitable to make medium-power laser modulators and self-pumped phase conjugators.[13-15] Previous research of some high-temperature phase-transition phenomena in niobates with TB structure has been performed.[2,16-21] However, the low-temperature properties of these crystals were hardly studied except for those of the $Ba_2NaNb_3O_5$ crystal.[22,23] In this work, dielectric, pyroelectric, thermal, and structural properties of these crystals at low temperatures were studied. It has been found that a new phase transition exists between 60 and 80 K, and it is different from the phase transition of $Ba_2NaNb_3O_{15}$ at 110 K reported in Refs. 22 and 23, where the polar axis was considered to remain in the c direction of the crystal cell.

II. EXPERIMENTS

A. Sample preparation

The crystals $(K_xNa_{1-x})_{0.4}(Sr_yBa_{1-y})_{0.8}Nb_2O_6$, $Sr_{1-x}Ba_xNb_2O_6$, and $Pb_xBa_{1-x}Nb_2O_6$ used for the measurements were grown by the Czochralski technique, and cut into two kinds of plates. The c plates were perpendicular to the c axis of the tetragonal cell and the a plates were perpendicular to the a axis of the tetragonal cell. After the gold electrodes were sputtered on the c faces, an electric field (2 kV/mm) was applied on the crystal samples in silicon oil at a temperature of 90 °C for poling. By confirming that the measured value of the piezoelectric constant d_{33} is saturated, the single-domain samples were then ready for measurement.

B. Measurement of dielectric constant

The dielectric constants and the tangent of the dielectric loss angle were measured by an impedance analyzer Hewlett-Packard HP-4192A. Samples were contacted close to the cooling head in a CSW-202 cryopump (Air Products, USA) and the temperature was controlled by APD-E with a Au-(Fe/Cr) thermoelement corrected by Air Products. The precision of the temperature measurement was ± 0.1 K (in the vicinity of 70 K), and the measuring frequencies were 100, 10, and 1 kHz. The measuring error of capacitance was less than 1% and that of the size of samples was less than 5%. The relative dielectric constants of the samples were calculated from the formula for a parallel-plate condenser. The results

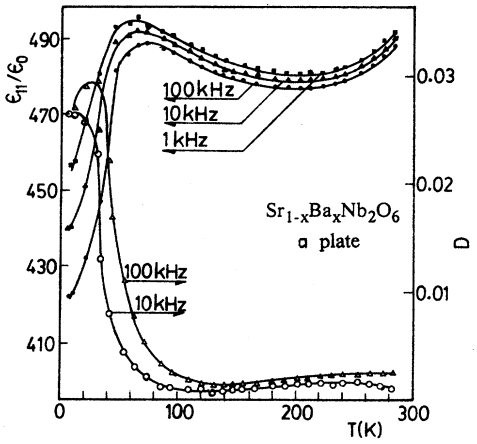

FIG. 1. The thermal anomaly of the dielectric properties for the a-plate sample of $Sr_{1-x}Ba_xNb_2O_6$ crystal at low temperature.

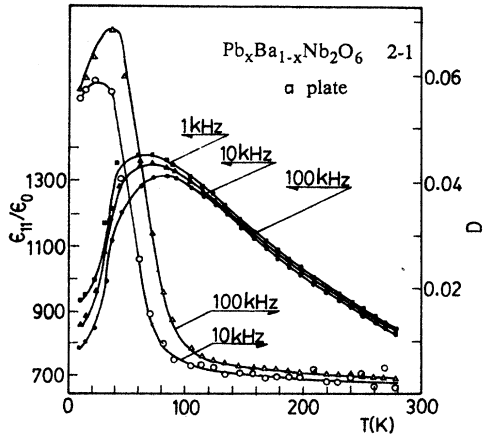

FIG. 2. The thermal anomaly of the dielectric properties for the a-plate sample of $Pb_xBa_{1-x}Nb_2O_6$ crystal at low temperature.

are shown in Figs. 1–6. The peak temperatures T_{max}, of the dielectric constant at different frequencies shown in Table I.

C. Measurement of pyroelectric properties

The control and measurement of temperature in the pyroelectric experiments are the same as those used in the measurement of dielectric constants mentioned above. A YD-01 integral electrical charge meter possessing sensitivity of 3.7×10^{-11} C per count was used to detect the change of charges in the sample as the temperature was changing. During the entire measurement process, the resistances of the samples were greater than 5×10^{10} Ω. The cooling and heating rates were about 3–5 K/min. The analytical procedure is as follows. A dc field (2.5 kV/mm) is first applied on the sample at 70 K, and the temperature of the sample is then lowered to 15 K. Then the sample is short-circuited for discharging. After discharging, the sample is connected to the integral charge meter in series. The pyroelectric charge was measured as the temperature was increased.

From the results of these experiments, we can see that the a plate of $(K_xNa_{1-x})_{0.4}(Sr_yBa_{1-y})_{0.8}Nb_2O_6$ has no pyroelectric effect if no electric field is applied at low temperatures, but has a fairly large effect when the field is applied. The c plate has only a weak effect, whether or not an electric field is applied. The measured results are shown in Figs. 7–11.

D. X-ray powder diffraction

X-ray powder diffraction analyses were performed at room temperature and at 85 K, respectively, with a diffraction angle 2θ varying from 15° to 60°. Polycrystalline samples were made from $(K_xNa_{1-x})_{0.4}$

TABLE I. The peak temperature T_{max}, of the dielectric constant and the onset temperature T_p, of the component of polarization along the tetragonal a axis in various crystal samples.

Composition of crystal samples	T_{max} (K) 1 kHz	10 kHz	100 kHz	T_p (K)
$Sr_{0.5}Ba_{0.5}Nb_2O_6$	60	64	73	58
1-1 (undoped)	80	90	98	84
$Pb_{0.37}Ba_{0.63}Nb_2O_6$				
2-1 (Doped)	68	74	84	64
$Pb_{0.30}Ba_{0.533}Nb_{0.306}Li_{0.028}Nb_2O_6$				
no. 1	58	68	86	80
$(K_{0.5}Na_{0.5})_{0.4}(Sr_{0.90}Ba_{0.10})_{0.8}Nb_2O_6$				
no. 2	60	68	80	76
$(K_{0.5}Na_{0.5})_{0.4}(Sr_{0.75}Ba_{0.25})_{0.8}Nb_2O_6$				
no. 3	58	70	76	~80
$(K_{0.5}Na_{0.5})_{0.4}(Sr_{0.60}Ba_{0.40})_{0.8}Nb_2O_6$				

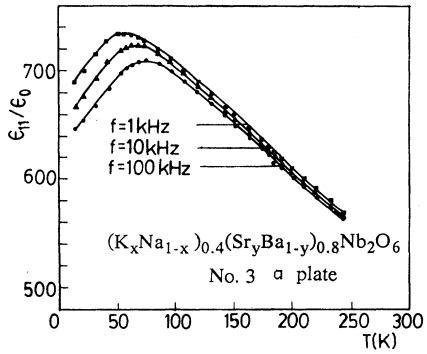

FIG. 3. The temperature dependence of the relative dielectric constant for the a-plate sample of $(K_xNa_{1-x})_{0.4}(Sr_yBa_{1-y})_{0.8}Nb_2O_6$ crystal.

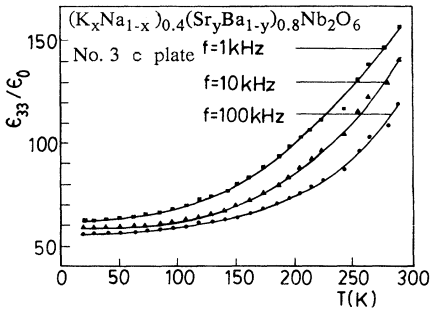

FIG. 5. The temperature dependence of the relative dielectric constant for the c-plate sample of $(K_xNa_{1-x})_{0.4}(Sr_yBa_{1-y})_{0.8}Nb_2O_6$ crystal.

$(Sr_yBa_{1-y})_{0.8}Nb_2O_6$ single crystals by grinding them into powder, annealing, and pressing into a plate, adding a bit of plastic binder. The crystal lattice parameters were $a=12.482$ Å and $c=3.954$ Å at room temperature, as determined data from the diffraction pattern.

E. Measurement of specific heat

The thermal conductivity of niobate crystals is smaller than that of copper by 2 orders of magnitude. For measurement of the specific heat, the time-constant method was used.[24] In order to limit temperature drift in the range of ± 0.005 K, two stages of temperature control were used. The mass of the sample was 304 mg, and the heating power was 0.655 mW. By using initial and boundary conditions, the specific heat of the sample was calculated from

$$c_p=(\pi/2)^2 m^{-1}(\tau/\Delta T)(dQ/dt)\ ,$$

where ΔT is the temperature difference before and after heating, dQ/dt is the heating power, τ is a time constant, and m is the mass of the sample.

III. RESULTS

A. Dielectric constant

Table I gives the compositions of the six crystals used in this work. The results of the dielectric-constant measurements for the a plate of $Sr_{1-x}Ba_xNb_2O_6$ are shown in Fig. 1. The curve of ϵ_{11}/ϵ_0 has a peak and the tangent of loss angle has a thermal anomaly in the vicinity of 60 K. The high-frequency dielectric constant is less than that of the low-frequency dielectronic constant. The peak temperature T_{max} of the dielectric constant for high frequency is higher than that for low frequency. This phase transition has a diffuse characteristic. For the c plate of $Sr_{1-x}Ba_xNb_2O_6$, the dielectric constant, ϵ_{33}/ϵ_0, monotonously decreases while the temperature comes down. The results for $Pb_xBa_{1-x}Nb_2O_6$ and $(K_xNa_{1-x})_{0.4}(Sr_yBa_{1-y})_{0.8}Nb_2O_6$ crystals are similar to those for $Sr_{1-x}Ba_xNb_2O_6$, as shown in Figs. 2–6.

B. Spontaneous polarization and pyroelectric coefficient

A peak occurs in the pyroelectric coefficient curve of the a plate in the vicinity of 60 K (see Figs. 7 and 8). This indicates that a component of spontaneous polariza-

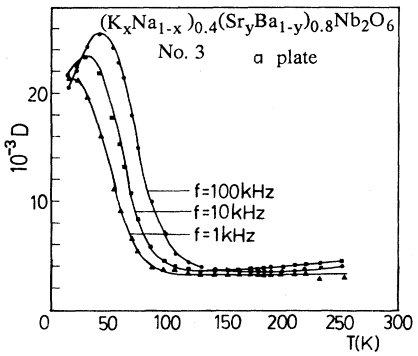

FIG. 4. The temperature dependence of the tangent of loss angle, D, for the a-plate sample of $(K_xNa_{1-x})_{0.4}(Sr_yBa_{1-y})_{0.8}Nb_2O_6$ crystal.

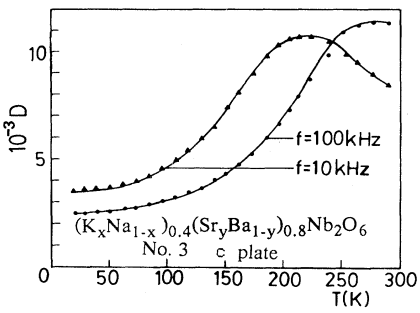

FIG. 6. The temperature dependence of the tangent of loss angle, D, for the c-plate sample of $(K_xNa_{1-x})_{0.4}(Sr_yBa_{1-y})_{0.8}Nb_2O_6$ crystal.

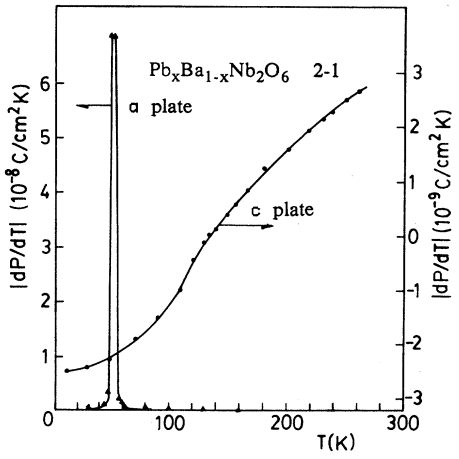

FIG. 7. The temperature dependence of the pyroelectric coefficients for $Pb_xBa_{1-x}Nb_2O_6$ crystal.

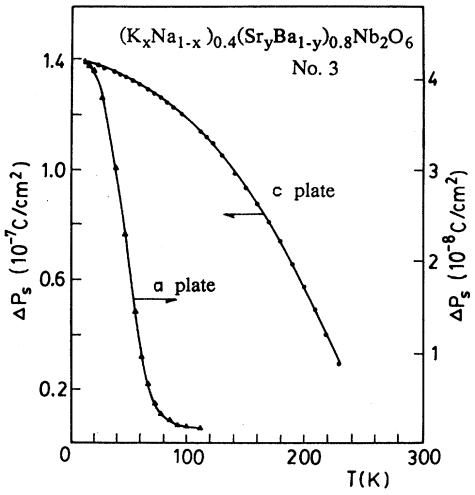

FIG. 9. The changes of the spontaneous polarization with the change of temperature for $(K_xNa_{1-x})_{0.4}(Sr_yBa_{1-y})_{0.8}Nb_2O_6$ crystal.

tions occurs at this temperature (see Fig. 9). However, for the *c* plate, in the absence of any peaks, the pyroelectric coefficients gradually reduce toward zero with a decrease of temperature. This means that P_s in the *c* direction changes very slowly, and it still has a large value at low temperatures. The temperature T_p, at which the onset of polarization component $P_{s(a)}$ along the *a* direction occurs when the *a*-plate sample was cooling down, was obtained by pyroelectric measurement (see Table I).

C. Direction of tilt of polarization axis

In order to determine the direction of the tilt of the polarization axis at low temperature, we cut a plate of crystal with major face to be perpendicular to the [110] direction of tetragonal cell in the $(K_xNa_{1-x})_{0.4}(Sr_yBa_{1-y})_{0.8}Nb_2O_6$ crystal and measured dielectric and pyroelectric properties of this plate sample. As shown in Figs. 10 and 11, the change of spontaneous polarization P_s of this (110) plate at the vicinity of transition temperature is obviously larger than that of the (100) face sample (i.e., the *a* plate), and the pyroelectric coefficient of the (110) plate is also larger than that of the (100) plate. When an electric field is applied to the (110) plate, and the change of spontaneous polarization in [1$\bar{1}$0] direction is measured in the vicinity of transition temperature, it can be observed that the change of spontaneous polarization in the [1$\bar{1}$0] direction is smaller by 1 order of magnitude than that in the [110] direction. This experiment indicates that the polarization axis in the low-temperature phase should be tilted towards the [110] direction of the tetragonal cell.

D. X-ray diffraction analyses

X-ray powder diffraction patterns of $(K_xNa_{1-x})_{0.4}(Sr_yBa_{1-y})_{0.8}Nb_2O_6$ at 298 and 85 K (Fig. 12) indicate

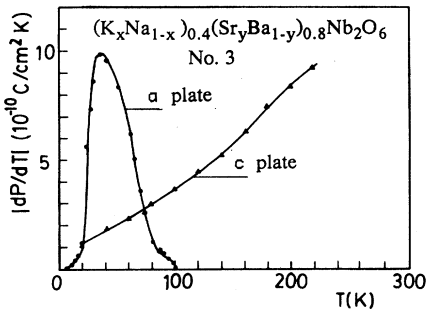

FIG. 8. The temperature dependence of the pyroelectric coefficients for $(K_xNa_{1-x})_{0.4}(Sr_yBa_{1-y})_{0.8}Nb_2O_6$ crystal.

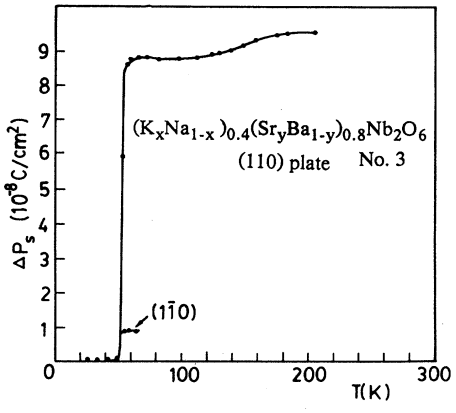

FIG. 10. The changes of the spontaneous polarization with the change of temperature for the (110) and (1$\bar{1}$0) face sample of KNSBN.

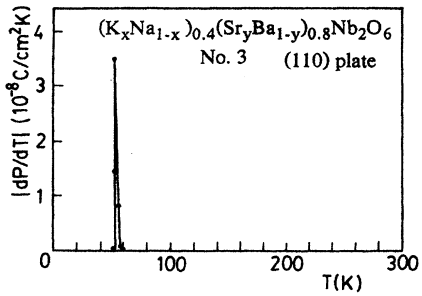

FIG. 11. The peak of pyroelectric coefficient along the [110] direction of tetragonal cell for $(K_xNa_{1-x})_{0.4}(Sr_yBa_{1-y})_{0.8}Nb_2O_6$.

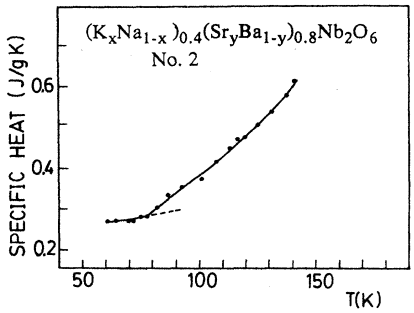

FIG. 13. The change of the specific heat with the change of temperature for $(K_xNa_{1-x})_{0.4}(Sr_yBa_{1-y})_{0.8}Nb_2O_6$ crystal.

that the diffraction peaks of (400) and (140) of point group $4mm$ at room temperature split at 85 K, and the diffraction peak (541) becomes stronger. This implies the initial appearance of the pseudo-orthorhombic phase. At 85 K, the lattice parameter $c=3.945$ Å. It has been shown that the phase transition has diffuse characteristics. From the changes of the dielectric constant and pyroelectric coefficient, the phase transition temperature is below 85 K. Based on the scanning electron microscopy (SEM) analyses of the composition fluctuation on microregions with 5000-Å size of diffuse phase transition,[25,26] the results of the x-ray analyses can be explained. In diffuse phase transition, the transition temperature of all microregions is different because of the fluctuation of composition in these regions. At 85 K, some of the microregions begin to transform. This makes the diffraction peaks of (400), (140), and (541) different from those at room temperature. When the tetragonal structure changes into a pseudo-orthorhombic structure, the split of the diffraction peak from (h,k,l) to (h',k',l') should occur. When the transition begins from the phase with $a=b$ to the phase with $a\neq b$, diffraction peaks which are easier to split are those whose Miller indices l are zero or small, and the difference between h and k is large. The peaks of (400) and (140) belong to this case.

Since the P_s possesses both of the components along the c axis and the b axis in the pseudo-orthorhombic cell, it could be suggested that the symmetry of the low-temperature phase belongs to point group m of the monoclinic structure, like some ferroelectrics, such as $Bi_4Ti_3O_{12}$.[27]

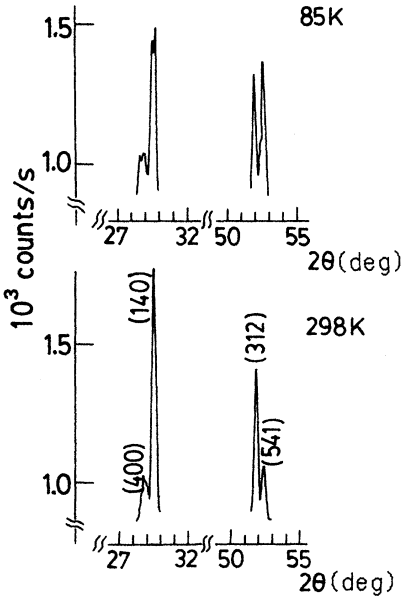

FIG. 12. X-ray diffraction patterns of $(K_xNa_{1-x})_{0.4}(Sr_yBa_{1-y})_{0.8}Nb_2O_6$ at 85 K (upper) and 298 K (lower).

E. Specific heat

Figure 13 gives the result of specific-heat measurements in $(K_xNa_{1-x})_{0.4}(Sr_yBa_{1-y})_{0.8}Nb_2O_6$ sample no. 2. No latent heat was observed in the range 40–140 K. The relative error is less than 5%. There is a change in the slope of the curve at 75–80 K, corresponding to the transition temperature.

IV. CONCLUSION AND DISCUSSION

From the experimental results, some conclusions are obtained as follows.

(1) A phase transition between 60 and 80 K, which has not previously been discovered, exists in $(K_xNa_{1-x})_{0.4}(Sr_yBa_{1-y})_{0.8}Nb_2O_6$, $Sr_{1-x}Ba_xNb_2O_6$, and $Pb_xBa_{1-x}Nb_2O_6$ crystals with tungsten-bronze-type structure. Dielectric constants and pyroelectric coefficients all have peaks near the phase transition temperature.

(2) From the splitting of x-ray diffraction peaks (400) and (140) at 85 K, it can be proven that the transition is from the tetragonal point group $4mm$ to the monoclinic point group m.

(3) Comparing the pyroelectric coefficients and the spontaneous polarizations along [100], [110], and [1$\bar{1}$0], it is indicated that this structure transition is a ferroelectric to ferroelectric (F-F) transition, and the direction of polarization axis tilts away by a small angle (less than a

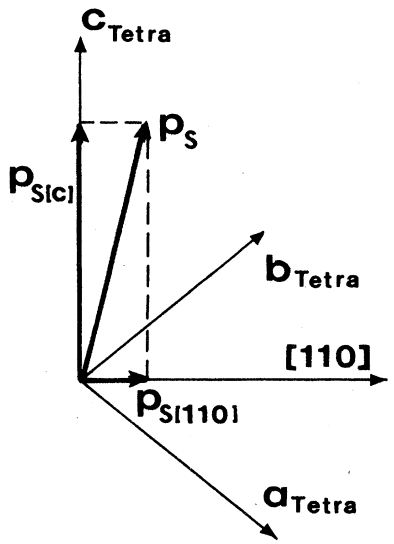

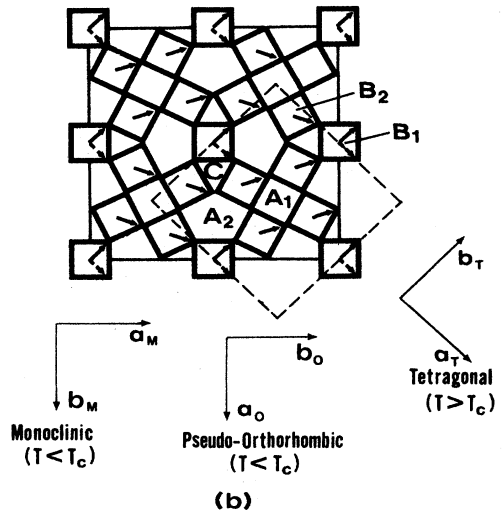

FIG. 14. A possible model for explaining that a component of P_s occurs along the a direction of the monoclinic cell when the temperature is below T_p. (a) P_s tilts away by a small angle from the c axis towards the [110] direction in the tetragonal structure. (b) The component of P_s occurs along the a direction of the monoclinic cell in tungsten-bronze structure (looking down the c axis of the pseudo-orthorhombic cell. A_1, A_2, B_1, B_2, and C represent different positions for cation's occupation).

few degrees) from [001] (i.e., the c-axis) towards the [110] direction of the tetragonal cell, i.e., the a axis of the monoclinic cell (or the b axis of the pseudo-orthorhombic cell). In contrast to the data of the phase transitions of $Ba_2NaNb_5O_{15}$ crystal reported in Refs. 22 and 23, this transition was discovered for the first time in $Sr_{1-x}Ba_xNb_2O_6$, $Pb_xBa_{1-x}Nb_2O_6$, and $(K_xNa_{1-x})_{0.4}(Sr_yBa_{1-y})_{0.8}Nb_2O_6$ crystals.

(4) No latent heat was observed from the result of specific-heat measurements. Thus the transition might belong to a higher-order phase transition.

(5) From the dielectric properties, one can see that the relative dielectric constant ϵ_{ij}/ϵ_0 at high frequency is smaller than that at low frequency. The tangent of the loss angle D and the peak temperature T_{max} of the dielectric constant at high frequency are higher than those at low frequency, and the dielectric constant peaks widen. This indicates that the transition is a diffuse phase transition.

The experimental results of $(K_xNa_{1-x})_{0.4}(Sr_yBa_{1-y})_{0.8}Nb_2O_6$, $Sr_{1-x}Ba_xNb_2O_6$, and $Pb_xBa_{1-x}Nb_2O_6$, which have the same structure, are very similar, so the transitions in these crystals are the same type. Figure 14 is a sketch projected along the c axis of a tungsten-bronze cell structure in which a tetragonal cell is shown by the dotted line and a monoclinic cell (or a pseudo-orthorhombic cell) is shown by the solid line. A possible model for explaining the component of P_s which occurs along the a axis of the monoclinic cell (i.e., the b axis of the pseudo-orthorhombic cell) is suggested (see Fig. 14). When the temperature is lower than T_p, the spontaneous polarization P_s tilts away by a small angle from the c axis towards the [110] direction of the tetragonal cell, i.e., the a axis of the monoclinic cell and the symmetry changes from point group $4mm$ to point group m.

There is a discrepancy between Fig. 9 and Fig. 10, i.e., Fig. 9 suggested a drop of 0.13 $\mu C/cm^2$ for the projection of P_s along the [001] direction, and a rise of 0.04 $\mu C/cm^2$ for that along the [100] direction on heating. Figure 10, on the other hand, suggests a rise of 0.087 $\mu C/cm^2$ along a [110] direction. These data are not enough to reconcile one to the other. It is believed that the discrepancy is caused by the deviation of the sample's orientation formed in the cutting process. However, these data are qualitatively reasonable for his model, because it is obvious that $|\Delta P_{s(c)}| > |\Delta P_{s[110]}| > |\Delta P_{s(a)}|$.

ACKNOWLEDGMENTS

This work was supported by The Science Fund of Chinese Academy of Sciences and by The Foundation of Advanced Research Center of Zhongshan University. The authors thank Professor Moses H. W. Chen and Dr. H. K. Kim at the Department of Physics, The Pennsylvania State University, for their assistance in some of the experiments.

[1]Takuro Ideka and Itaru Fujimura, Jpn. J. Appl. Phys. **13**, 57 (1974).
[2]A. M. Glass, J. Appl. Phys. **40**, 4699 (1969).
[3]Chen Huanchu and Xu Yuhuan, Physics **10**, 729 (1981).
[4]Xu Yuhuan and Chen Huanchu, Acta Scientiarum Naturalium Universitatis Sunyatseni, **2**, 52 (1982).
[5]Chen Huanchu and Xu Yuhuan, J. Chin. Sil. Soc. **10**, 406 (1982).
[6]Chen Huanchi and Xu Yuhuan, Acta Scientiarum Naturalium Universitatis Sunyatseni, **2**, 57 (1982).
[7]Xu Yuhuan and Chen Huanchu, Acta Phys. Sinica **32**, 706 (1983),
[8]Xu Yuhuan, Chen Huanchu, and L. E. Cross, Ferroelectrics **54**, 123 (1984).
[9]Xu Yuhuan, Chen Huanchu, and L. E. Cross, Ferroelectrics Lett. **2**, 189 (1984).
[10]Xu Yuhuan and Chen Huanchu, Acta Phys. Sinica **34**, 978 (1985).
[11]Xu Yuhuan, Chen Huanchu, and S. T. Liu, Jpn. J. Appl. Phys. Suppl. **24-2**, 278 (1985).
[12]Chen Ting and Xu Yuhuam, J. Chin. Sil. Soc. **15**, 544 (1987).
[13]R. R. Neurgaonkar *et al.*, J. Cryst. Growth **84**, 629 (1987).
[14]M. D. Ewband *et al.*, J. Appl. Phys. **62**, 374 (1987).
[15]J. Rodriguez *et al.*, Appl. Opt. **26**, 1732 (1987).
[16]P. B. Jamieson *et al.*, J. Chem. Phys. **50**, 4352 (1969).
[17]P. B. Jamieson *et al.*, J. Chem. Phys. **48**, 5048 (1969).
[18]J. C. Toledano and J. Schneck, Solid State Commun. **16**, 1101 (1975).
[19]J. Burgeat and J. C. Toledano, Solid State Commun. **20**, 281 (1976).
[20]K. L. Ngai and T. L. Reinecke, Phys. Rev. Lett. **38**, 74 (1977).
[21]V. A. Isupov, Ferroelectrics Lett. **7**, 7 (1987).
[22]J. Schneck *et al.*, Solid State Commun. **21**, 57 (1977).
[23]Takuro Ikeda, Jpn. J. Appl. Phys. **13**, 1065 (1974).
[24]R. Bachmann, Rev. Sci. Instrum. **43**, 205 (1972).
[25]G. A. Smolensky, J. Phys. Soc. Jpn. **28**, 26 (1970).
[26]Yuhuan Xu and Hong Wang, Jpn. J. Appl. Phys. Suppl. **24-2**, 236 (1985).
[27]S. E. Cummins and L. E. Cross, Appl. Phys. Lett. **10**, 14 (1967).